








# Experimental resin infiltrant with antibacterial activity and ionic release: *in-vitro* study

Layla Karine Oliveira Silva<sup>1</sup> , Ana Ferreira Souza<sup>1\*</sup> ,  
May Anny Alves Fraga<sup>2</sup> , Priscila Regis Matos  
Pedreira<sup>3</sup> , Américo Bortolazzo Correr<sup>2</sup> , Flávio  
Henrique Baggio Aguiar<sup>1</sup> , Giselle Maria Marchi<sup>1</sup> 

<sup>1</sup> Department of Restorative Dentistry, Faculdade de Odontologia de Piracicaba (FOP), Universidade Estadual de Campinas (UNICAMP), Piracicaba, São Paulo, Brazil.

<sup>2</sup> Department of Dental Materials, Faculdade de Odontologia de Piracicaba (FOP), Universidade Estadual de Campinas (UNICAMP), Piracicaba, São Paulo, Brazil.

<sup>3</sup> Professor Jorge Amado University Center, Salvador, Bahia, Brazil.

## Corresponding author:

Ana Ferreira Souza  
Avenida Limeira, 901, Piracicaba – SP, Brazil. Zip code: 13414-903  
Phone: (+55) 098 98191-4015.  
Fax: (+55) 019 2106-5218  
E-mail: fsana.ufma@gmail.com

**Editor:** Dr. Altair A. Del Bel Cury

**Received:** October 10, 2023

**Accepted:** June 18, 2024



**Objective:** To assess the influence of the combination of the antibacterial monomer dimethylaminohexadecyl methacrylate (DMAHDM) and amorphous calcium phosphate nanoparticles (NACP) on the antibacterial and ion release potentials, as well as the physical properties of experimental resin infiltrants.

**Methodology:** The study comprised the following groups: ERI (Pure Experimental Resin Infiltrant [ERI]: 75% TEGDMA + 25% BisEMA, 0.5% camphorquinone [CQ], and 1% ethyl 4-dimethylaminobenzoate [EDMAB]); ERIDM (ERI + 3% DMAHDM), ERINACP (ERI + 1.5% NACP), and ERIDM\_NACP (ERI + 3% DMAHDM + 1.5% NACP). From samples of each group, Degree of Conversion (DC; n=6) and Sorption and Solubility (SO/SOL; n=8) were assessed. The antibacterial potential was evaluated through biomass accumulation (BA; n=6) and bacterial metabolism (BM; n=6) assays after cultivating *Streptococcus mutans* biofilm on the materials. Ionic release (IR; n=3) of Ca<sup>2+</sup> and PO<sub>4</sub><sup>(3-)</sup> from the groups after 7, 14, and 28 days of immersion was also analyzed. Data were analyzed for normality and homoscedasticity, and statistical analysis was performed using appropriate tests with a significance level of 5%. **Results:** For DC, ERIDM showed no statistical difference from ERI. ERI had the lowest means of SO/SOL, and ERIDM\_NACP had the highest. ERIDM exhibited no statistical difference from ERI. For BM, ERIDM and ERIDM\_NACP had the lowest means. ERINACP and ERIDM\_NACP exhibited ionic release during the analyzed period. **Conclusions:** The resin infiltrant containing DMAHDM and NACP exhibits potent antibacterial activity against *S. mutans* and Ca<sup>2+</sup> and PO<sub>4</sub><sup>(3-)</sup> ionic release.

**Keywords:** Dental caries. Tooth remineralization. Anti-bacterial agents.

## Introduction

Tooth decay is one of the most common diseases affecting people all over the world<sup>1</sup>. It is the result of a continuous process of interaction between cariogenic bacteria that produce acid and fermentable carbohydrates, forming bacterial biofilm, as well as factors from the host itself, such as microbiota, hygiene, salivation, and diet<sup>2</sup>. The first visible clinical manifestation of the disease is characterized by a white spot lesion with a porous and non-cavitated appearance<sup>2</sup>. Its development occurs through the process of demineralization in tooth enamel, resulting from acid attack by biofilm-forming bacteria accumulated on its surface<sup>2</sup>.

Ideally, caries lesions should be detected early, as at this stage it is still possible to promote their remineralization through non-invasive treatments such as fluoridation or the application of remineralizing components<sup>3</sup>. For areas that are more difficult to access and for patients who do not cooperate with oral hygiene, a good option is the use of resin infiltrants<sup>4</sup>.

Treatment with resinous infiltration is a microinvasive approach to help manage initial caries lesions. Its application does not require a prior session for tooth separation or wear of dental tissue, and several systematic reviews indicate its superiority in controlling the progression of interproximal carious lesions compared to isolated non-invasive treatments<sup>4-6</sup>.

Resin infiltrant consists of a low-viscosity material that penetrates the porosities of initial caries lesions, significantly increasing resistance against further demineralization. By filling the lesion, a mechanical barrier is formed against the diffusion of bacterial acids<sup>3</sup>. Resin infiltration is effective against the development of new carious lesions and the halting of existing ones<sup>3</sup>, and its effectiveness in controlling the progression of early interproximal carious lesions was reported in a randomized clinical trial with 7 years of follow-up<sup>5</sup>.

However, resin infiltrants have some limitations, such as the inability to seal all porosities of initial caries lesions and allowing biofilm accumulation on their surface due to their resinous nature<sup>7,8</sup>. They are mainly composed of the triethylene glycol dimethacrylate (TEGDMA) monomer, which is significantly hydrophilic and susceptible to degradation in the oral cavity<sup>9</sup>.

In an effort to overcome these shortcomings, the incorporation of therapeutic agents into the infiltrant has been investigated<sup>10-13</sup>, such as dimethylaminohexadecyl methacrylate (DMAHDM), an antibacterial quaternary ammonium monomer that has been shown to be effective against caries-related bacteria<sup>10-13</sup>. Quaternary ammonium monomers form covalent bonds with the polymer matrix and are immobilized in resin materials, resulting in sustained efficacy<sup>11-13</sup>. Its incorporation into these materials has led to satisfactory physical-mechanical properties and inhibition of bacterial biofilm, in addition to an anti-demineralization effect<sup>11-13</sup>.

Another approach that is currently being investigated is the incorporation of bioactive particles into the infiltrant to give the material the potential to release ions into the surrounding environment<sup>12-14</sup>. One example is Nanoparticulate Amorphous Calcium

Phosphate (NACP), which shows positive results when incorporated into resin materials, acting as an acid neutralizer and releasing calcium and phosphate ions into the surrounding environment, thus serving as an auxiliary agent against the development of secondary carie<sup>11-15</sup>.

In previous studies, the combination of DMAHDM and NACP in resin materials was investigated, obtaining even more satisfactory results, with reduced bacterial growth and high concentrations of calcium and phosphate ion release<sup>15-16</sup>. Given the reported benefits of DMAHDM and NACP, it is worth investigating whether the combination of these agents could promote therapeutic effects in the resin infiltrant, thus contributing to reducing the chance of recurrent caries lesions. No equivalent investigation has been identified in the literature; therefore, the aim of this study was to evaluate the physical properties, antibacterial potential and ion release potential of an experimental enamel infiltrant containing the DMAHDM monomer and/or NACP particles.

The null hypotheses tested were that 1) The incorporation of DMAHDM and/or NACP would not cause changes in the physical properties tested compared to the control experimental infiltrant; 2) The incorporation of DMAHDM alone or in combination with NACP would not exhibit antibacterial effects compared to the control experimental infiltrant, and 3) The incorporation of NACP alone or in combination with DMAHDM would not promote ionic release compared to the control experimental infiltrant.

## Materials and Methods

### Formulation of experimental resin infiltrants

The infiltrants were prepared in a laboratory with yellow lighting and temperature controlled at 25°C. The experimental infiltrants had a monomeric base consisting of a mixture of 75% by weight of triethylene glycol dimethacrylate (TEGDMA) and 25% by weight of bisphenol-A dimethacrylate ethoxylated (BisEMA), as well as 0.5% by weight of camphorquinone (CQ) and 1% of ethyl 4-dimethylamino-benzoate (EDMAB). This monomer composition was divided into a group of pure Experimental Resin Infiltrant (ERI), ERI + DMAHDM 3% (ERIDM), ERI + NACP 1.5% (ERINACP) and ERI + DMAHDM 3% + NACP 1.5% (ERIDM\_NACP) (Table 1). The reagents were purchased from Sigma-Aldrich (Steinheim, Germany). The components of the groups were weighed on a precision analytical balance (AUW220D Shimadzu, Kyoto, Japan), handled and mixed on a magnetic stirrer until completely homogeneous. The infiltrants were stored in black polyethylene containers and kept refrigerated.

**Table 1.** Groups followed by their composition according to the therapeutic agents employed, by weight.

Group	Composition
ERI	98.5% TEGDMA + BisEMA base; 0.5% CQ; 1% EDMAB
ERIDM	95.5% TEGDMA + BisEMA base; 0.5% CQ; 1% EDMAB; 3% DMAHDM
ERINACP	97% TEGDMA + BisEMA base; 0.5% CQ; 1% EDMAB; 1.5% NACP
ERIDM_NACP	94% TEGDMA + BisEMA base; 0.5% CQ; 1% EDMAB; 3% DMAHDM; 1.5% NACP

ERI: Pure Experimental. ERIDM: Experimental + 3% DMAHDM. ERINACP: Experimental + 1.5% NACP. ERIDM\_NACP: Experimental + 3% DMAHDM + 1.5% NACP. TEGDMA = triethylene glycol dimethacrylate, BisEMA = ethoxylated isfenol A glycidyl dimethacrylate, CQ = camphorquinone, EDMAB = ethyl 4-(dimethylamino) benzoate, DMAHDM = dimethylaminohexadecyl methacrylate, NACP = nanoparticles of amorphous calcium phosphate.

## Degree of Conversion

The degree of conversion was analyzed using Fourier Transform Infrared Spectroscopy associated with Attenuated Total Reflectance (FTIR-ATR; MIRacle, Pike Technologies, Inc. Madison, WI, USA). The unpolymerized material ( $n = 6$ ; 110  $\mu$ l) was dispensed using a precision pipette (Microraman M25, Gilson Medical Electronics S.A., France) directly onto the ATR device crystal coupled to the FTIR, and the initial spectrum was obtained (32 scans, resolution of 4<sup>-1</sup>cm). Subsequently, photoactivation was performed for 40 s (1000 mW/cm<sup>2</sup> of irradiance; Valo Corded; Ultradent, South Jordan, UT, USA), and immediately after, the new spectrum of the polymerized material was obtained.

The calculation of the degree of conversion was performed by the ratio of absorption bands at 1610 cm<sup>-1</sup> and 1637 cm<sup>-1</sup>, using the formula:  $DC = (1 - \text{area of final peak} / \text{area of initial peak}) \times 100\%$ <sup>17</sup>.

## Water Sorption and Solubility

The ISO 4049/2009 specifications were followed, except for the sample dimensions<sup>17</sup>. Discs of the materials (5 mm diameter x 1 mm in thickness,  $n = 8$ ) were made from silicone matrices (Express XT Putty Soft-VPS; 3M ESPE, St. Paul, MN, USA). The materials were added and photopolymerized under an LED light source for 60 s (irradiance of 1000 mW/cm<sup>2</sup>; Valo, Ultradent). Subsequently, the discs were deposited in a desiccator containing silica gel and stored in an oven at 37°C. Daily weighing was carried out, every 24 hours, on a precision analytical balance (Shimadzu – AUW220D, Tokyo, Japan), until constant mass values (M1) were obtained, with a variation of less than 0.002 g.

After obtaining M1, volume values (mm<sup>3</sup>) of the samples were obtained from the averages of individual thickness and diameter measurements, obtained with the aid of a digital caliper (Mitutoyo, Kanagawa, Japan). Subsequently, the samples were stored in closed Eppendorf tubes containing 1.43 ml of distilled water at 37°C for seven days. After this period, the Eppendorf tubes were removed from the incubator and kept at room temperature for 30 minutes. After being washed under running water and gently dried with absorbent paper, the samples were reweighed on an analytical balance to obtain M2. Once this value was obtained, the samples were stored again and weighed

every 24 hours until a new constant mass value (M3) was reached. The following formulas were used to calculate the values of SO and SOL:

$$SO = \frac{(M2 - M3)}{V} \quad SOL = \frac{(M1 - M3)}{V}$$

### Biofilm biomass accumulation assay

Test specimens (n = 6) were prepared in the form of discs (5mm in diameter x 2 mm in thickness), following the same procedure as described above. The specimens were polished with silicon carbide paper of grit #1200 and #2000 to standardize the surface roughness (CarbiMet 2; Buehler, Lake Bluff, IL, USA) on a rotary polisher (Arotec SA Indústria e Comércio Ltda; Cotia, SP, Brazil) under cooling to standardize the surface roughness.

A strain of *Streptococcus mutans* (UA159) was used to promote the formation of bacterial biofilm on the specimens from each group. The specimens were placed in devices and placed in the wells of polystyrene microculture plates. Each well contained 300  $\mu$ l of bacterial suspension at  $10^8$  CFU/mL (adjusted to 0.1; 660 nm), 150  $\mu$ l of 20% sucrose solution, and 2.550  $\mu$ l of Brain Heart Infusion (BHI) agar medium. An incubation period of 48 hours was used for biofilm formation and development, with a medium change after 24 hours<sup>13</sup>.

After 48 hours, the specimens were washed with phosphate-buffered saline (PBS) and placed in a 24-well plate containing 1 mL of 100% methanol for 15 minutes for fixation<sup>13</sup>. Subsequently, the specimens were washed again with PBS and transferred to another 24-well plate containing 1 mL of 0.1% crystal violet solution for five minutes. The specimens were washed with PBS to remove residual dye. Then, the discs were transferred to a new 24-well plate and 2 mL of 95% ethanol solution was added to each well, and the plate was agitated horizontally at 80 rpm for 45 minutes at room temperature<sup>13</sup>.

The ethanol solution (100  $\mu$ L) from each well was diluted with 95% ethanol solution to 200  $\mu$ L and transferred to a 96-well plate. A microplate reader (ASYS-UVM 340, Biochrom Ltd, Cambridge, UK) was used to measure the absorbance of the solution at 595 nm OD<sup>13</sup>.

### Bacterial metabolism assay

The specimen preparation (n = 6) and the cultivation of *S. mutans* biofilm were carried out as described above. After 48 hours of cultivation, the discs were washed with PBS and transferred to 24-well plates containing 2 ml of MTT (3-[4,5-dimethylthiazol-2-yl]-2,5-diphenyltetrazolium bromide) at 0.5mg/ml per well and incubated for 1 hour at 37°C in 5% CO<sub>2</sub>. Then, the discs were transferred to another 24-well plate with 2 mL of dimethyl sulfoxide (DMSO) in each well and incubated under horizontal shaking (80 rpm) at room temperature for 20 minutes to dissolve the formazan crystals. Subsequently, 200  $\mu$ l of this solution from each well was transferred to a 96-well plate, and the OD 540nm was determined using a microplate reader (ASYS-UVM 340, Biochrom Ltd, Cambridge, UK)<sup>13</sup>.

## Ionic Release

The analysis of ionic release was performed only for the groups that contained NACP in the composition. Specimens from groups ERINACP and ERIDM\_NACP (5 mm in diameter x 1 mm in thickness, n = 3 per group) were prepared as described above. The specimens were stored dry for 24 hours and individually stored in 10 g of deionized water. After 7, 14, and 28 days of immersion, the entire volume of the medium was collected and filtered using a nylon syringe filter (0.45  $\mu\text{m}$ ) and acidified using 10  $\mu\text{m}$  of concentrated nitric acid. The concentration of calcium and phosphorus ions in the immersion solution was determined using inductively coupled plasma optical emission spectrometry (ICP-OES, Agilent Technologies, Santa Clara, CA, USA)<sup>18</sup>.

## Statistical Analysis

The data was analyzed for normality (Shapiro-Wilk test,  $p > 0.05$ ) and homoscedasticity (Levene test,  $p > 0.05$ ), and then submitted to the appropriate tests. Data that met the assumptions of normality and homoscedasticity were submitted to ANOVA and Tukey's *post-hoc* test. Data that met the assumption of normality, but not homoscedasticity, were submitted to Welch's ANOVA and Games-Howell *post-hoc* tests. The significance level applied was 5% (IBM Corp. Released 2011. IBM SPSS Statistics for Windows, Version 20.0. Armonk, NY: IBM Corp).

For Degree of conversion and Sorption, One-way ANOVA and Tukey *post-hoc* tests were performed. For Solubility, Biofilm biomass accumulation and Bacterial metabolism assays, Welch's ANOVA and Games-Howell *post-hoc* tests were applied. For  $\text{Ca}^{2+}$  ion release, the data showed normal distribution and homoscedasticity, so they were subjected to a Two-way ANOVA test (Group x time) and Bonferroni *post-hoc* test.

## Results

**Table 2.** Mean and standard deviation (sd) of Degree of Conversion (%), Sorption ( $\mu\text{g}/\text{mm}^3$ ), Solubility ( $\mu\text{g}/\text{mm}^3$ ), Biofilme Biomass Accumulation and Bacterial Metabolism (Absorbance; nm), by group.

Variable	Infiltrant				p-value
	ERI	ERIDM	ERINACP	ERIDM_NACP	
Degree of conversion (%)	59.94 (0.62) AB	62.46 (2.38) A	57.43 (1.90) CB	56.59 (1.45) C	< 0.001
Sorption ( $\mu\text{g}/\text{mm}^3$ )	77.3 (4.45) D	112 (4.09) B	95.6 (3.82) C	120 (3.83) A	< 0.001
Solubility ( $\mu\text{g}/\text{mm}^3$ )	3.49 (1.77) D	38.4 (5.19) B	18 (2.46) C	64.4 (14.8) A	< 0.001
Biofilme Biomass (nm)	0.591 (0.242) ABC	0.253 (0.0237) C	0.469 (0.0440) A	0.309 (0.0105) B	0.002
Bacterial Metabolism (nm)	0.241 (0.015) B	0.124 (0.003) C	0.328 (0.055) A	0.133 (0.01) C	< 0.001

Different letters indicate statistical difference between the columns.

For Degree of Conversion, ERI and ERIDM exhibited the highest averages, not differing from each other ( $p < 0,001$ ). ERI differed from ERIDM\_NACP ( $p = 0.014$ ) and ERIDM differed from ERINACP and ERIDM\_NACP ( $p < 0.001$ ). For sorption and solubility, ERI exhibited the lowest averages and all groups differed from each other ( $p < 0.01$ ).

For Biomass accumulation, ERIDM, ERINACP and ERIDM\_NACP differed from each other, but did not differ from ERI ( $p < 0.01$ ). For Bacterial Metabolism, ERIDM and ERIDM\_NACP presented the lowest means, not differing from each other ( $p = 0.247$ ). ERI differed from all groups (ERIDM  $p < 0.001$ ; ERINACP  $p = 0.037$ ; ERIDM\_NACP  $p < 0.001$ ), as well as ERINACP (ERI  $p = 0.037$ ; ERIDM  $p = 0.001$ ; ERIDM\_NACP  $p = 0.001$ ).

In the ion release test, for  $\text{PO}_4^{(3-)}$  release, detectable release was identified by the applied methodology (limit of quantification = 0.10 ppm) only at the 7-day evaluation, for both groups, with an average release of 0.247 mg/L in ERINACP and 0.316 mg/L in ERIDM\_NACP. For ionic  $\text{Ca}^{2+}$  release, there was no difference between ERINACP and ERIDM\_NACP at different times ( $p > 0.05$ ). Comparing the different evaluation times within each group, within ERINACP there was a difference between 7 and 28 days ( $p = 0.026$ ), with the highest  $\text{Ca}^{2+}$  release occurring in 7 and the lowest in 28 days. In ERIDM\_NACP, the 7-day release was the highest, statistically differing from 14 ( $p = 0.035$ ) and 28 days ( $p = 0.018$ ). 14 and 28 days did not differ from each other in either group.

The values of  $\text{Ca}^{2+}$  ion release are expressed in Chart 01.

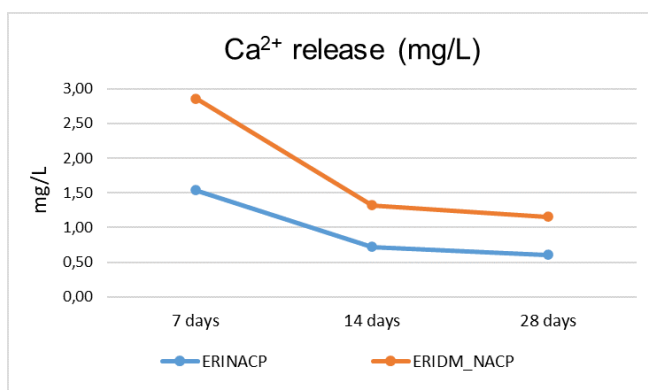


**Chart 01.**  $\text{Ca}^{2+}$  ion release (mg/L) for each group in the different evaluation periods.

## Discussion

This study evaluated the incorporation of an antibacterial compound, the quaternary ammonium monomer dimethylaminohexadecyl methacrylate (DMAHDM), and a bioactive particle, nanoparticulate amorphous calcium phosphate (NACP), into an experimental resin infiltrant, aiming to develop an optimized infiltrant with antimicrobial activity and ion release. The first null hypothesis was rejected, as the incorporation of 1.5% NACP (ERINACP and ERIDM\_NACP) resulted in a reduction in the

degree of conversion compared to the group containing only DMAHDM (ERIDM), and the incorporation of both investigated agents increased the sorption and solubility of the materials compared to the control (ERI). The second null hypothesis was also rejected, as the incorporation of DMAHDM significantly reduced the accumulation of biomass and bacterial metabolism of *S. mutans* compared to groups without the monomer (ERI and ERINACP). Similarly, the third null hypothesis was rejected, as the incorporation of NACP into the infiltrant promoted the release of  $\text{Ca}^{2+}$  and  $\text{PO}_4^{(3-)}$  ions into the medium.

The degree of conversion test is crucial to determine the efficiency of material polymerization, which directly influences the properties of the final product. The degree of conversion corresponds to the consumption of aliphatic double bonds during monomeric polymerization<sup>19</sup>. A high degree of conversion is associated with increased bonding between polymeric chains, resulting in a stronger and more durable material<sup>20</sup>. Additionally, a higher degree of conversion leads to a harder material, improving resistance to deformation and wear<sup>21</sup>.

In this study, it is observed that group ERIDM, containing DMAHDM, presented the highest values, with no statistical difference from the control group. DMAHDM has the ability to copolymerize, covalently bonding to the resin matrix, thereby justifying its non-detrimental effect on the degree of conversion of the infiltrant<sup>10-16,18-27</sup>. Previous studies that investigated the incorporation of 3% of the monomer into experimental composite resins indicated that the incorporation did not compromise fracture toughness and microhardness properties of the resulting materials<sup>15,23</sup>.

In a recently published literature review, most analyzed studies also did not identify impairment to the mechanical properties of resulting materials, such as flexural strength, surface roughness, dentin bond strength, color stability, and the aforementioned fracture toughness and microhardness, after incorporating fractions of 1.5 to 3.75% by weight of DMAHDM<sup>22</sup>. The cited review also included studies that analyzed the surface roughness of materials containing 3-5% DMAHDM and reported that incorporation did not compromise the property, even after biofilm challenges<sup>22</sup>.

On the other hand, group ERINACP, containing NACP, showed a lower average with no statistical difference from the control group, and group ERIDM\_NACP, containing both therapeutic agents, presented the lowest average among the groups, differing only from ERINACP. NACP particles were added to the infiltrant without prior silanization to avoid compromising the intended ionic release. This nonsilanization may be responsible for the detriment to the formed polymeric network, which may have favored water infiltration between chains and leaching of unreacted monomers<sup>12,24,25</sup>, possibly related to higher rates of sorption and solubility for groups containing the agent. The addition of bioactive particles increases the hydrophilicity of resinous compounds<sup>12,25,26</sup>.

For Water Sorption and Solubility, a significant increase was observed in all groups containing the therapeutic agents. ERIDM and ERINACP, which contain DMAHDM and NACP individually, respectively, showed significantly higher averages than the pure experimental infiltrant, ERI. ERIDM\_NACP presented the highest averages,

indicating that sorption and solubility become even higher when the compounds are associated.

The sorption values are related to how hydrophilic the infiltrant is. In this study, the elevation of values can be explained by the addition of components to the experimental infiltrant. DMAHDM belongs to the category of quaternary ammonium salt (QAS) monomers<sup>27</sup>, which are polar and hydrophilic molecules, and the polarity of the composite seems to dictate water absorption, so it can be expected that the more DMAHDM molecules, the more hydrophilic the composite and, therefore, this hydrophilicity associated with the heterogeneity of the composite containing QAS can increase water sorption<sup>27</sup>. Another related factor may be the lower quality of the polymeric network formed in the presence of nonsilanized particles, as was the case with NACP<sup>12,25</sup>. These results may imply a compromise in the strength of the resulting material<sup>9</sup>, which can affect clinical performance due to the environment in which the restorative material will be placed, the oral cavity.

The addition of both agents, whether associated or not, also resulted in an increase in solubility, which may be related to the dissolution of particles in the aqueous medium, as previously reported for resin-based materials containing bioactive particles<sup>12,24,25</sup>, as well as particle detachment from the matrix due to nonsilanization. This chemical degradation is associated with oxidation and hydrolysis processes that occur in the presence of water<sup>21</sup>. However, for ionic release to occur through the addition of NACP, there must be solubility in the material.

ERI presented the lowest water sorption and solubility values and differed from the other groups, indicating a higher quality of the polymeric network formed in the absence of therapeutic agents. A variety of chemical and physical processes is directly related to sorption and solubility. These processes can produce deleterious effects, such as volumetric, physical, and chemical changes in the structure and function of polymers<sup>21,27</sup>. High water absorption swells the polymer network and causes leaching of unreacted monomers. The results of this study corroborate with previous reports where the incorporation of QAS and bioactive particles increased sorption and solubility<sup>25,27</sup>.

Bacterial biofilm biomass accumulation was evaluated using a method based on biofilm staining with crystal violet. Crystal violet is a basic dye that binds to negatively charged surface molecules and polysaccharides in the extracellular matrix<sup>28</sup>. In this assay, crystal violet is used as an indicator of bacterial growth<sup>28</sup>. The procedure involves exposing the groups to a medium containing bacteria and assessing the antibacterial potential of each group's components, where the bacteria are treated and incubated with a crystal violet solution, which is absorbed by live bacterial cells and adheres to the surface of the cell membrane<sup>28</sup>. The color intensity associated with the bacteria is measured by spectrophotometry<sup>29</sup>. Higher absorbance averages indicate a higher biomass quantity, i.e., lower antibacterial activity, while a reduction in color intensity is associated with bactericidal activity<sup>29</sup>.

It was observed that group ERIDM had the lowest average, indicating that biofilm adherence to the samples was lower than in the other groups, demonstrating greater bactericidal activity. ERIDM statistically differed from ERINACP and

ERIDM\_NACP; however, it did not show a statistical difference from ERI, as well as ERINACP and ERIDM\_NACP, which is due to the high standard deviation of this group. Among the groups containing therapeutic agents, ERINACP (1.5% NACP) showed the highest biomass accumulation, statistically differing from the groups containing DMAHDM. Next is group ERIDM\_NACP, which showed lower accumulation compared to ERINACP but still higher than ERIDM, which contained only DMAHDM. These results may indicate that the addition of NACP may have slightly decreased the antibacterial capacity of the component, as there was a higher dilution of the infiltrant components.

According to the study by Wang et al., which used 3% DMAHDM, similar to group ERIDM, the biofilm biomass in composites containing DMAHDM was much lower than in composites without DMAHDM. These results are also evident in the studies by Wu et al. and Zhou et al., both of which conducted live/dead staining assays. In Wu et al.'s study, the results showed that in composites containing 0.75%, 1.5%, 2.25%, and 3% DMAHDM, respectively, the number of dead bacteria increased as the percentage of DMAHDM increased, while in the control group, which had only 20% NACP, the biofilm was mostly alive<sup>24</sup>. In Zhou et al.'s study, it was shown that groups containing 3% DMAHDM and 3% DMAHDM + 30% NACP had substantial dead bacteria for all tested species, while the group containing only 30% NACP and the control group were covered with live bacteria<sup>30</sup>.

The bacterial metabolism assay is a colorimetric assay that measures the enzymatic reduction of MTT (3-[4,5-dimethylthiazol-2-yl]-2,5-diphenyltetrazolium bromide). This assay is based on the ability of living cells to reduce MTT to formazan, an insoluble product that imparts an intense purple color<sup>31</sup>. The quantification of absorbance obtained in the MTT assay allows estimating cell viability since the amount of formed formazan is directly related to the number of live cells. Higher absorbance indicates a higher concentration of formazan, meaning higher metabolic activity in the biofilm<sup>23</sup>. The results showed that ERIDM and ERIDM\_NACP, which contain the antibacterial monomer DMAHDM, presented the lowest absorbance values, exhibiting lower metabolic activity of the *S. mutans* bacteria.

The results of the present study corroborate with the study by Xie et al., where NACP and DMAHDM were added to a composite resin of bisphenol A ethoxylated dimethacrylate (EBPADMA) and pyromellitic glycerol dimethacrylate (PMGDM). The groups containing lower or no percentage of DMAHDM showed higher metabolic activity in *S. mutans* biofilms, while those containing the antibacterial monomer exhibited lower metabolic activity. In the cited study, a percentage of metabolic activity inversely proportional to the DMAHDM percentage of each group is demonstrated. The first group, which did not contain the monomer, showed higher metabolic activity, the second group had 1.5% DMAHDM, hence intermediate metabolic activity, and the third group containing 3% DMAHDM exhibited lower metabolic activity than all others<sup>32</sup>.

Similar results were also reported in the study by Xiao et al., where NACP and DMAHDM were added to a resin consisting of pyromellitic glycerol dimethacrylate (PMDGDM) and bisphenol A ethoxylated dimethacrylate (EBPADMA). Groups containing 3% DMAHDM exhibited lower metabolic activity in the biofilm of *P. gingivalis*, *A.*

*actinomycetemcomitans*, and *F. nucleatum* compared to groups without the monomer. Group 1 containing 30% NACP + 3% MPC + 3% DMAHDM and Group 2 containing 30% NACP + 3% MPC + 3% DMAHDM + 0.12% AgNPs showed lower biofilm metabolic activity for all three tested bacterial species in the study compared to groups containing 30% NACP and a commercial compound called Renamel Microfill, significantly reducing the CFU counts for all these three species<sup>33</sup>.

The QAMs' reported mechanism of action is based on the electrostatic interaction between their positively charged ( $N^+$ ) sites and the negatively charged bacterial cell, which causes a disturbance in the electrical balance of the cell membrane, causing the bacteria to die due to its own osmotic pressure<sup>34</sup>. In addition, due to their long chain length, QAMs can perforate the bacterial cell wall, compromising its physical integrity and releasing its cellular content<sup>34</sup>. The DMAHDM monomer has an alkyl chain length of 16, and has been shown to have stronger antibacterial activity than other QAMs with shorter chain lengths<sup>35</sup>.

The ion release test aimed to evaluate the release capacity of calcium ions ( $Ca^{2+}$ ) and phosphorus ( $PO_4^{(3-)}$ ) in the surrounding medium, which could help prevent the formation of recurrent caries lesions by strengthening the adjacent enamel<sup>18</sup>. The method used for analysis in this study detected  $PO_4^{(3-)}$  ion release only during the 7-day immersion period, so future studies should use other methods for this analysis.

For  $Ca^{2+}$  release, there was no difference between ERINACP and ERIDM\_NACP in the different evaluation periods. In relation to the different evaluation periods within each group, ERINACP showed greater release in the shortest period (7 days) and lower release after a longer period (28 days). The same was observed for the ERIDM\_NACP group, with greater release at 7 days compared to 14 and 18 days. For both groups, there was no difference in the release that occurred after 14 or 28 days of immersion.

The reduction in calcium release after the 7-day period is commonly observed in compounds with  $Ca^{2+}$  ion release, as was observed in the study by Campos et al., where approximately less than 10% of the total calcium mass is released<sup>18</sup>. This may occur because only molecules near the surface are responsible for releasing  $Ca^{2+}$  ions. If the material were incorporated in a thin layer, such as in cavity lining, the percentage of ion release would be higher<sup>18</sup>.

Previous studies suggest that the release of mineral ions can promote remineralization of adjacent tooth tissue<sup>11,15</sup>. NACP acts as an acid neutralizer and releases calcium and phosphate ions into the surrounding environment, promoting remineralization, making it an auxiliary agent against the development of secondary caries<sup>11,15</sup>. Melo et al. observed in a previous study that the association of therapeutic agents used in the present study had a positive effect on the performance of restorative resin materials, as it reduced the cariogenic impact of bacterial biofilm, improving the resistance to mechanical and acid challenges of materials in the oral environment<sup>11</sup>.

Based on the results obtained within the limitations of the present study, it was observed that experimental resin infiltrants containing DMAHDM and NACP exhibited antimicrobial activity against *S. mutans* and released  $Ca^{2+}$  and  $PO_4^{(3-)}$  ions into the medium, which could contribute to the creation of an unfavorable environment for the development of recurrent caries lesions at the margins of the material.

Future studies should investigate the ability of these materials to penetrate initial caries lesions in dental enamel, as well as the duration of these antimicrobial and ion release effects.

In conclusion, the incorporation of the DMAHDM monomer, either individually or associated with NACP, demonstrated a significant inhibition of bacterial viability in the experimental resin infiltrants. Moreover, the incorporation of NACP promoted the release of calcium ions ( $\text{Ca}^{2+}$ ) and phosphate ions ( $\text{PO}_4^{3-}$ ) into the surrounding medium. Nonetheless, it should be noted that the introduction of these agents compromised the sorption and solubility characteristics of the material.

## Author Contribution

**Layla Karine Oliveira Silva:** Conceptualization, Methodology, Formal analysis, Investigation, Resources, Writing - Original Draft, Writing - Review & Editing, Visualization, Funding acquisition; **Ana Ferreira Souza:** Conceptualization, Methodology, Formal analysis, Investigation, Resources, Writing - Original Draft, Writing - Review & Editing, Visualization, Funding acquisition; **May Anny Alves Fraga:** Methodology, Writing - Review & Editing; **Priscila Regis Matos Pedreira:** Methodology, Writing - Review & Editing; **Américo Bortolazzo Correr:** Methodology and Project administration; **Flávio Henrique Baggio Aguiar:** Methodology and Project administration; **Giselle Maria Marchi:** Conceptualization, Resources, Writing - Review & Editing, Supervision, Project administration and Funding acquisition. All authors made a significant contribution to the work reported, whether that is in the conception, study design, execution, acquisition of data, analysis and interpretation, or in all these areas; took part in drafting, revising or critically reviewing the article; gave final approval of the version to be published; have agreed on the journal to which the article has been submitted; and agree to be accountable for all aspects of the work.

---

## References

1. GBD 2017 Disease and Injury Incidence and Prevalence Collaborators. Global, regional, and national incidence, prevalence, and years lived with disability for 354 diseases and injuries for 195 countries and territories, 1990-2017: a systematic analysis for the Global Burden of Disease Study 2017. *Lancet*. 2018 Nov;392(10159):1789-858. doi: 10.1016/S0140-6736(18)32279-7. Erratum in: *Lancet*. 2019 Jun;393(10190):e44. doi: 10.1016/S0140-6736(19)31047-5.
2. Kidd EA, Fejerskov O. What constitutes dental caries? Histopathology of carious enamel and dentin related to the action of cariogenic biofilms. *J Dent Res*. 2004;83 Spec No C:C35-8. doi: 10.1177/154405910408301s07.
3. Urquhart O, Tampi MP, Pilcher L, Slayton RL, Araujo MWB, Fontana M, et al. Nonrestorative treatments for caries: systematic review and network meta-analysis. *J Dent Res*. 2019 Jan;98(1):14-26. doi: 10.1177/0022034518800014. Epub 2018 Oct 5.
4. Chen Y, Chen D, Lin H. Infiltration and sealing for managing non-cavitated proximal lesions: a systematic review and meta-analysis. *BMC Oral Health*. 2021 Jan;21(1):13. doi: 10.1186/s12903-020-01364-4.
5. Paris S, Bitter K, Krois J, Meyer-Lueckel H. Seven-year-efficacy of proximal caries infiltration - Randomized clinical trial. *J Dent*. 2020 Feb;93:103277. doi: 10.1016/j.jdent.2020.103277.

6. Elrashid AH, Alshaiji BS, Saleh SA, Zada KA, Baseer MA. Efficacy of resin infiltrate in noncavitated proximal carious lesions: a systematic review and meta-analysis. *J Int Soc Prev Community Dent*. 2019 May-Jun;9(3):211-8. doi: 10.4103/jispcd.JISPCD\_26\_19.
7. Nedeljkovic I, De Munck J, Slomka V, Van Meerbeek B, Teughels W, Van Landuyt KL. Lack of buffering by composites promotes shift to more cariogenic bacteria. *J Dent Res*. 2016 Jul;95(8):875-81. doi: 10.1177/0022034516647677.
8. Yim HK, Min JH, Kwon HK, Kim BI. Modification of surface pretreatment of white spot lesions to improve the safety and efficacy of resin infiltration. *Korean J Orthod*. 2014 Jul;44(4):195-202. doi: 10.4041/kjod.2014.44.4.195.
9. Fonseca AS, Labruna Moreira AD, de Albuquerque PP, de Menezes LR, Pfeifer CS, Schneider LF. Effect of monomer type on the CC degree of conversion, water sorption and solubility, and color stability of model dental composites. *Dent Mater*. 2017 Apr;33(4):394-401. doi: 10.1016/j.dental.2017.01.010.
10. Clarin A, Ho D, Soong J, Looi C, Ipe DS, Tadakamadla SK. The antibacterial and remineralizing effects of biomaterials combined with DMAHDM nanocomposite: a systematic review. *Materials (Basel)*. 2021 Mar;14(7):1688. doi: 10.3390/ma14071688.
11. Melo MA, Orrego S, Weir MD, Xu HH, Arola DD. Designing multiagent dental materials for enhanced resistance to biofilm damage at the bonded interface. *ACS Appl Mater Interfaces*. 2016 May;8(18):11779-87. doi: 10.1021/acsami.6b01923.
12. Souza AF, Souza MT, Damasceno JE, Ferreira PVC, Alves de Cerqueira G, Baggio Aguiar FH, et al. Effects of the incorporation of bioactive particles on physical properties, bioactivity and penetration of resin enamel infiltrant. *Clin Cosmet Investig Dent*. 2023 Mar;15:31-43. doi: 10.2147/CCIDE.S398514.
13. Yu J, Huang X, Zhou X, Han Q, Zhou W, Liang J, et al. Anti-caries effect of resin infiltrant modified by quaternary ammonium monomers. *J Dent*. 2020 Jun;97:103355. doi: 10.1016/j.jdent.2020.103355.
14. Andrade Neto DM, Carvalho EV, Rodrigues EA, Feitosa VP, Sauro S, Mele G, et al. Novel hydroxyapatite nanorods improve anti-caries efficacy of enamel infiltrants. *Dent Mater*. 2016 Jun;32(6):784-93. doi: 10.1016/j.dental.2016.03.026.
15. Bhadila G, Wang X, Zhou W, Menon D, Melo MAS, Montaner S, et al. Novel low-shrinkage-stress nanocomposite with remineralization and antibacterial abilities to protect marginal enamel under biofilm. *J Dent*. 2020 Aug;99:103406. doi: 10.1016/j.jdent.2020.103406.
16. Balhaddad AA, Ibrahim MS, Weir MD, Xu HH, Melo MAS. Concentration dependence of quaternary ammonium monomer on the design of high-performance bioactive composite for root caries restorations. *Dent Mater*. 2020 Aug;36(8):e266-8. doi: 10.1016/j.dental.2020.05.009.
17. Mathias C, Gomes RS, Dressano D, Braga RR, Aguiar FHB, Marchi GM. Effect of diphenyliodonium hexafluorophosphate salt on experimental infiltrants containing different diluents. *Odontology*. 2019 Apr;107(2):202-8. doi: 10.1007/s10266-018-0391-0. Epub 2018 Oct 1.
18. Campos AL, Vela BF, Pires Silva Borges L, Trinca RB, Pfeifer CS, Braga RR. Compositional boundaries for functional dental composites containing calcium orthophosphate particles. *J Mech Behav Biomed Mater*. 2023 Aug;144:105928. doi: 10.1016/j.jmbbm.2023.105928.
19. Dai Z, Xie X, Zhang N, Li S, Yang K, Zhu M, et al. Novel nanostructured resin infiltrant containing calcium phosphate nanoparticles to prevent enamel white spot lesions. *J Mech Behav Biomed Mater*. 2022 Feb;126:104990. doi: 10.1016/j.jmbbm.2021.104990. Epub 2021 Nov 23.
20. Leprince JG, Palin WM, Hadis MA, Devaux J, Leloup G. Progress in dimethacrylate-based dental composite technology and curing efficiency. *Dent Mater*. 2013 Feb;29(2):139-56. doi: 10.1016/j.dental.2012.11.005. Epub 2012 Nov 27. Erratum in: *Dent Mater*. 2013 Apr;29(4):493.

21. Ferracane JL. Hygroscopic and hydrolytic effects in dental polymer networks. *Dent Mater.* 2006 Mar;22(3):211-22. doi: 10.1016/j.dental.2005.05.005. Epub 2005 Aug 8.
22. Duarte de Oliveira FJ, Ferreira da Silva Filho PS, Fernandes Costa MJ, Rabelo Caldas MRG, Dutra Borges BC, Gadelha de Araújo DF. A comprehensive review of the antibacterial activity of dimethylaminohexadecyl methacrylate (DMAHDM) and its influence on mechanical properties of resin-based dental materials. *Jpn Dent Sci Rev.* 2021 Nov;57:60-70. doi: 10.1016/j.jdsr.2021.03.003.
23. Wu J, Zhou H, Weir MD, Melo MA, Levine ED, Xu HH. Effect of dimethylaminohexadecyl methacrylate mass fraction on fracture toughness and antibacterial properties of CaP nanocomposite. *J Dent.* 2015 Dec;43(12):1539-46. doi: 10.1016/j.jdent.2015.09.004.
24. Jardim RN, Rocha AA, Rossi AM, de Almeida Neves A, Portela MB, Lopes RT, Pires Dos Santos TM, et al. Fabrication and characterization of remineralizing dental composites containing hydroxyapatite nanoparticles. *J Mech Behav Biomed Mater.* 2020 Sep;109:103817. doi: 10.1016/j.jmbbm.2020.103817.
25. Yang SY, Piao YZ, Kim SM, Lee YK, Kim KN, Kim KM. Acid neutralizing, mechanical and physical properties of pit and fissure sealants containing melt-derived 45S5 bioactive glass. *Dent Mater.* 2013 Dec;29(12):1228-35. doi: 10.1016/j.dental.2013.09.007.
26. Misra SK, Mohn D, Brunner TJ, Stark WJ, Philip SE, Roy I, et al. Comparison of nanoscale and microscale bioactive glass on the properties of P(3HB)/Bioglass composites. *Biomaterials.* 2008 Apr;29(12):1750-61. doi: 10.1016/j.biomaterials.2007.12.040.
27. Vidal ML, Rego GF, Viana GM, Cabral LM, Souza JPB, Silikas N, et al. Physical and chemical properties of model composites containing quaternary ammonium methacrylates. *Dent Mater.* 2018 Jan;34(1):143-51. doi: 10.1016/j.dental.2017.09.020. Epub 2017 Nov 10.
28. Wang L, Melo MA, Weir MD, Xie X, Reynolds MA, Xu HH. Novel bioactive nanocomposite for Class-V restorations to inhibit periodontitis-related pathogens. *Dent Mater.* 2016 Dec;32(12):e351-61. doi: 10.1016/j.dental.2016.09.023.
29. Mataraci E, Dosler S. In vitro activities of antibiotics and antimicrobial cationic peptides alone and in combination against methicillin-resistant *Staphylococcus aureus* biofilms. *Antimicrob Agents Chemother.* 2012 Dec;56(12):6366-71. doi: 10.1128/AAC.01180-12.
30. Zhou W, Peng X, Zhou X, Weir MD, Melo MAS, Tay FR, et al. In vitro evaluation of composite containing DMAHDM and calcium phosphate nanoparticles on recurrent caries inhibition at bovine enamel-restoration margins. *Dent Mater.* 2020 Oct;36(10):1343-55. doi: 10.1016/j.dental.2020.07.007.
31. Mosmann T. Rapid colorimetric assay for cellular growth and survival: application to proliferation and cytotoxicity assays. *J Immunol Methods.* 1983 Dec;65(1-2):55-63. doi: 10.1016/0022-1759(83)90303-4.
32. Xie X, Wang L, Xing D, Arola DD, Weir MD, Bai Y, et al. Protein-repellent and antibacterial functions of a calcium phosphate rechargeable nanocomposite. *J Dent.* 2016 Sep;52:15-22. doi: 10.1016/j.jdent.2016.06.003.
33. Xiao S, Wang H, Liang K, Tay F, Weir MD, Melo MAS, et al. Novel multifunctional nanocomposite for root caries restorations to inhibit periodontitis-related pathogens. *J Dent.* 2019 Feb;81:17-26. doi: 10.1016/j.jdent.2018.12.001. Epub 2018 Dec 12.
34. Rego GF, Vidal ML, Viana GM, Cabral LM, Schneider LFJ, Portela MB, et al. Antibiofilm properties of model composites containing quaternary ammonium methacrylates after surface texture modification. *Dent Mater.* 2017 Oct;33(10):1149-56. doi: 10.1016/j.dental.2017.07.010.
35. Zhou H, Li F, Weir MD, Xu HH. Dental plaque microcosm response to bonding agents containing quaternary ammonium methacrylates with different chain lengths and charge densities. *J Dent.* 2013 Nov;41(11):1122-31. doi: 10.1016/j.jdent.2013.08.003.